# The effect of scale and interfacial tension on liquid–liquid dispersion in in-line Silverson rotor–stator mixers

Hall, Steven; Pacek, Andrzej W.; Kowalski, Adam J.; Cooke, Mike; Rothman, David

*DOI:*
10.1016/j.cherd.2013.04.021

Contents lists available at ScienceDirect

Chemical Engineering Research and Design

journal homepage: www.elsevier.com/locate/cherd

# The effect of scale and interfacial tension on liquid–liquid dispersion in in-line Silverson rotor–stator mixers☆

Steven Hall[a,*], Andrzej W. Pacek[a], Adam J. Kowalski[b], Mike Cooke[c], David Rothman[d]

[a] School of Chemical Engineering, University of Birmingham, Birmingham B15 2TT, UK
[b] Unilever R&D, Port Sunlight, Laboratory Bebington, Wirral, CH63 3JW, UK
[c] School of Chemical Engineering and Analytical Science, University of Manchester, Manchester, M60 1QD, UK
[d] Silverson Machines Ltd., Chesham, Buckinghamshire, HP5 1PQ, UK

ABSTRACT

The effect of scale, processing conditions, interfacial tension and viscosity of the dispersed phase on power draw and drop size distributions in three in-line Silverson rotor–stator mixers was investigated with the aim to determine the most appropriate scaling up parameter. The largest mixer was a factory scale device, whilst the smallest was a laboratory scale mixer. All the mixers were geometrically similar and were fitted with double rotors and standard double emulsor stators. 1 wt.% silicone oils with viscosities of 9.4 mPa s and 339 mPa s in aqueous solutions of surfactant or ethanol were emulsified in single and multiple pass modes. The effect of rotor speed, flow rate, dispersed phase viscosity, interfacial tension and scale on drop size distributions was investigated.

It was found that for all three scales, power draw is the sum of the rotor and flow contributions, with proportionality constants, $Po_Z$ and $k_1$, that are practically scale independent. Sauter mean drop size appeared to correlate better with tip speed than energy dissipation rate. For ethanol/water solutions, mean drop size correlated well with Weber number based on interfacial tension, but for surfactant solutions effective interfacial tension gave better correlations with Weber number.



*Keywords:* Rotor–stator mixer; Emulsification; Scale-up; Tip speed; Energy dissipation rate; Weber number

## 1. Introduction

Mixing of two or more immiscible liquids to form a stable emulsion is an important processing step in the manufacture of products such as shampoos, salad dressings, bitumen, pharmaceuticals and many others, and is commonly carried out in in-line high shear rotor–stator mixers. In-line rotor–stator mixers are attractive as they can combine multiple process operations, and they may be used in continuous processing in a single pass mode or batch processing in a multiple pass mode.

Despite the widespread application of in-line rotor–stator mixers, the current understanding of their performance is still rather limited. Frequently, the development of new emulsion-based products is based on experience, and process parameters are typically selected by trial and error at increasing scales. To accurately scale-up emulsification in rotor–stator mixers it is important to understand the effect of process and formulation parameters on droplet size to predict and control the characteristic properties of multiphase products from the laboratory scale through to the manufacturing scale.

The first step in scaling up of high shear mixers is to determine the power draw necessary to accomplish the required degree of emulsification in two-phase systems. The full expression for power draw in turbulent flow is given by (Baldyga et al., 2007; Cooke et al., 2008; Kowalski, 2009):

$$P = Po_Z \rho N^3 D^5 + k_1 M N^2 D^2 \quad (1)$$



* *Corresponding author*. Tel.: +31 104605052.
E-mail address: steven.hall@unilever.com (S. Hall).

Received 29 November 2012; Received in revised form 15 April 2013; Accepted 19 April 2013
0263-8762/$ – see front matter © 2013 The Institution of Chemical Engineers. Published by Elsevier B.V. All rights reserved.
http://dx.doi.org/10.1016/j.cherd.2013.04.021

**Nomenclature**

*Symbols*

| | |
|---|---|
| $A, A_1 \ldots A_x$ | constants |
| $A_F$ | fraction of outer stator open area |
| $A_h$ | area of stator holes/openings ($m^2$) |
| $A_s$ | surface area of stator ($m^2$) |
| $B$ | number of batch vessel turnovers |
| $b, b_1 \ldots b_x$ | exponents |
| $C, C_1 \ldots C_x$ | dimensionless empirical constants |
| $C_p$ | specific heat capacity at constant pressure ($J\,(kg\,K)^{-1}$) |
| $D$ | rotor diameter (outer rotor) (m) |
| $D_{r,i}$ | inner rotor diameter (m) |
| $D_{r,o}$ | outer rotor diameter (m) |
| $D_{s,i}$ | inner stator diameter (m) |
| $D_{s,o}$ | outer stator diameter (m) |
| $d$ | droplet diameter (m) |
| $d_{0,1}$ | diameter below which 10% of the sample population reside (m) |
| $d_{0,5}$ | number median diameter (m) |
| $d_{0,9}$ | diameter below which 90% of the sample population reside (m) |
| $d_{32}$ | volume surface mean diameter (Sauter mean drop diameter) (m) |
| $d_{max}$ | maximum stable drop diameter (m) |
| $E_0$ | Gibbs elasticity ($N\,m^{-1}$) |
| $E_{sd}$ | surface dilational modulus ($N\,m^{-1}$) |
| $E_V$ | energy density ($J\,m^{-3}$) |
| $f_V$ | continuous volume frequency distribution |
| $HI$ | homogenisation index |
| $h_r$ | rotor height (m) |
| $h_s$ | stator height (m) |
| $k_1$ | 'flow' power constant |
| $M$ | mass flow rate ($kg\,s^{-1}$) |
| $N$ | rotor speed ($s^{-1}$) |
| $n_{b,i}$ | number of inner rotor blades |
| $n_{b,o}$ | number of outer rotor blades |
| $n_h$ | number of stator holes |
| $n_{hr}$ | number of stator holes per row |
| $n_r$ | number of stator rows |
| $P$ | power (W) |
| $P_h$ | perimeter of stator openings (m) |
| $P_T$ | 'torque on rotor shaft' power term (W) |
| $p$ | pressure (Pa) |
| $\Delta p$ | pressure difference across the mixing head (Pa) |
| $Po_Z$ | 'zero flow' power constant |
| $Q$ | volumetric flow rate (impeller pumping capacity) ($m^3\,s^{-1}$) |
| $R^2$ | coefficient of determination |
| $s$ | skewness for a log-normal distribution |
| $t$ | time (s) |
| $t_D$ | diffusion adsorption time scale (s) |
| $t_{def}$ | droplet deformation time scale (s) |
| $t_m$ | mixing time (s) |
| $t_R$ | total residence time in the mixing head (s) |
| $U_T$ | tip speed ($m\,s^{-1}$) |
| $V_H$ | volume of mixing head (swept outer rotor volume) ($m^3$) |
| $V_h$ | homogenisation volume ($m^3$) |
| $V_T$ | volume of mixing tank ($m^3$) |
| $w$ | span for a log-normal distribution |
| $x, x_1, x_2$ | exponents |
| $y, y_1, y_2$ | exponents |

*Greek symbols*

| | |
|---|---|
| $\beta$ | constant |
| $\Gamma$ | surface excess concentration ($g\,m^{-2}$) |
| $\varepsilon$ | mean energy dissipation rate per unit mass of fluid ($W\,kg^{-1}$) |
| $\varepsilon_T$ | 'torque on rotor shaft' energy dissipation rate per unit mass of fluid ($W\,kg^{-1}$) |
| $\eta_K$ | Kolmogoroff's length scale of turbulence (m) |
| $\theta$ | temperature (K) |
| $\theta_b$ | temperature due to bearing friction (K) |
| $\theta_c$ | temperature correction between the temperature probes (K) |
| $\Delta\theta$ | temperature difference across the mixing head (K) |
| $\mu$ | fluid viscosity (Pa s) |
| $\mu_c$ | continuous phase viscosity (Pa s) |
| $\mu_d$ | dispersed phase viscosity (Pa s) |
| $\rho$ | fluid density ($kg\,m^{-3}$) |
| $\rho_c$ | continuous phase density ($kg\,m^{-3}$) |
| $\rho_d$ | dispersed phase density ($kg\,m^{-3}$) |
| $\sigma$ | surface/interfacial tension ($N\,m^{-1}$) |
| $\sigma_{eff}$ | effective interfacial tension ($N\,m^{-1}$) |
| $\sigma_{rms}$ | root mean squared difference |
| $\tau$ | residence time (s) |
| $\tau_s$ | cohesive surface tension stresses ($kg\,m^{-1}\,s^{-2}$) |
| $\tau_v$ | cohesive viscous stresses ($kg\,m^{-1}\,s^{-2}$) |

*Dimensionless groups*

| | |
|---|---|
| $N_c$ | circulation number, $\frac{Qt_m}{V_T}$ |
| $N_Q$ | flow number, $\frac{Q}{ND^3}$ |
| $Po$ | power number, $\frac{P}{\rho N^3 D^5}$ |
| $Re$ | Reynolds number, $\frac{\rho ND^2}{\mu}$ |
| $We$ | Weber number, $\frac{\rho_c N^2 D^3}{\sigma}$ |
| $We_{eff}$ | effective Weber number, $\frac{\rho_c N^2 D^3}{\sigma_{eff}}$ |

Eq. (1) has been validated for pilot plant (Kowalski et al., 2011) and small scale (Hall et al., 2011) Silverson mixers.

Expressions for Sauter mean diameter have been reported for a range of formulations and processing equipment, with most of the previous work summarised by Leng and Calabrese (2004). In many practical applications of geometrically similar devices it is convenient to correlate Sauter mean diameter with energy dissipation rate per unit mass or rotor tip speed:

$$d_{32} \propto \varepsilon^{b_1} \tag{2}$$

$$d_{32} \propto U_T^{b_2} \tag{3}$$

Theoretical correlations for maximum stable drop size in turbulent liquid–liquid dispersions are based on mechanistic models (Hinze, 1955), which assume that drops are broken if the disruptive stress is greater than the cohesive stress (Leng and Calabrese, 2004). The disruptive stress is related to energy dissipation rate calculated within a cascade model of homogeneous isotropic turbulence. In dilute liquid–liquid systems with low viscosity dispersed phases, viscous stresses are negligible and only cohesive forces due to interfacial tension

stabilise the drop. In turbulent flow, assuming that ($d_{32}/d_{max}$) is constant and that drops are larger than Kolmogoroff's length scale, average stable drop size ($d_{32}$), can be related to the local energy dissipation rate (Leng and Calabrese, 2004):

$$d_{32} = C_1\left(\frac{\sigma}{\rho_c}\right)^{3/5}\varepsilon^{-2/5} \quad (4)$$

The constant $C_1$ is of the order of one (Davies, 1985). For turbulent flow conditions, in geometrically similar systems, Eq. (4) can be rearranged to:

$$\frac{d_{32}}{D} = C_2 We^{-3/5} \quad (5)$$

Eq. (5) is frequently used for scaling emulsification processes in stirred vessels where the constant $C_2$ varies from 0.09 to 0.125 depending on impeller type and *Po* (Pacek et al., 1999). Calabrese et al. (2000) applied Eq. (5) to correlate the Sauter mean diameter in a batch high shear rotor–stator mixer and reported a constant of 0.040.

In the case of very viscous dispersed phases, internal viscous stresses resisting droplet deformation become more important than surface stresses, and for drops larger than Kolmogoroff's length scale, average drop size can be calculated from (Leng and Calabrese, 2004):

$$d_{32} = C_3(\rho_c\rho_d)^{-3/8}\mu_d^{3/4}\varepsilon^{-1/4} \quad (6)$$

Equations derived for different breakage mechanisms are summarised in Table 1 (Leng and Calabrese, 2004; Padron, 2005).

The accuracy of the Hinze model can be improved by accounting for the effect of intermittency on disruptive stresses acting on drops (Baldyga et al., 2001). However determination of the multi-fractal scaling exponent and the relationship between this exponent and proportionality functions is limited to large volumes of liquid, therefore it might have limited application in high shear mixers.

The above models were developed and frequently used for stirred vessels. However, Colenbrander (2000) claimed that drop size in stirred vessels cannot be correlated with energy dissipation rate and Okufi et al. (1990) and El-Hamouz et al. (2009) suggested tip speed as an appropriate scaling up parameter.

Information on scaling up of rotor–stator mixers in open literature is limited. Maa and Hsu (1996) examined emulsification in a Virtishear homogeniser and reported that drops of ~1 μm size were produced above 10,000 rpm at the large scale and above 15,000 rpm at the small scale, however they did not discuss scale-up parameters. Kamiya et al. (2010a) examined an IKA Works Inc. small mixer ($D$ = 0.031 m) and a large mixer ($D$ = 0.057 m) with 0.25 mm rotor–stator gaps. They recommended 'homogenisation index' (*HI*) based on the local energy dissipation rate and the 'circulation number' ($N_c$):

$$HI = \left(\frac{P}{\rho V_h}\right)N_c \quad (13)$$

$$N_c = \left(\frac{Q}{V_T}\right)t_m \quad (14)$$

for estimating mean droplet diameter for different batch sizes, rotor speeds and mixer geometry configurations:

$$d_{0.5} = HI^{-0.328} \quad (15)$$

Kamiya et al. (2010b) examined a pilot scale ($D$ = 0.198 m) and a production scale rotor–stator mixer ($D$ = 0.396 m) and correlated mean droplet size with total energy dissipation rate and claimed that such scaling up does not require geometric similarity, constant tip speed or constant gap width.

Mean drop size in in-line (continuous) rotor–stator mixers can also be correlated with energy density which accounts for the effect of flow rate and the mode of operation (single or multiple passes) (Karbstein and Schubert, 1995):

$$d_{32} \propto E_V^{b_3} \propto (\varepsilon t_R)^{b_4} \quad (16)$$

with $b_3$~−0.35 for turbulent inertial forces and ~−0.75 for turbulent shear forces (Schubert and Engel, 2004).

Manufacturers often design and scale-up rotor–stator mixers based on equal rotor tip speed, since the nominal shear rate in the rotor–stator gap is constant, when the gap width remains equal on scale-up (Atiemo-Obeng and Calabrese, 2004).However, findings from Francis (1999) and Thapar (2004) suggest that tip speed is better for correlating drop size than shear rate in the gap.

In this work, emulsification of silicone oils of vastly different viscosity in three geometrically similar in-line rotor–stator mixers of different sizes (from the lab to the factory scale) was investigated. Power draw and average drop size/drop size distributions have been measured and experimental drop sizes correlated with different scaling parameters. Since interfacial tension is an important parameter in droplet break-up, its effect on drop size was investigated by using solutions of ethanol as continuous phases, and by employing surfactant solutions at different concentrations. This study significantly builds on previous work (Hall et al., 2011) by investigating a factory scale device, and the effect of single and multiple passes and interfacial tension on drop size distributions.

## 2. Materials and methods

### 2.1. Equipment

The Silverson rotor–stator mixers (Silverson Machines Ltd., Chesham, UK) investigated in this work were three scales of in-line device; the laboratory scale 088/150 UHS, pilot plant scale 150/250 MS and factory scale 450/600 UHS models (Fig. 1 and Table 2). All mixers comprised of double rotors, enclosed within standard double Silverson emulsor screens (Fig. 1). The rotor–stator gap width was 0.24 mm, the stator thickness was 2.0 mm, and the stators contained 1.59 mm diameter holes on a triangular pitch at all scales.

The design of each stator was geometrically similar but there were minor differences in the rotor design. However, experiments show that the design/type of the rotor has only a marginal effect on drop size distributions.

The experimental rig enabling investigation of single pass and multiple pass emulsification is described in detail elsewhere (Hall et al., 2011). Coarse emulsions were prepared in an 800 L mixing tank for the single pass experiments and a 60 L tank for the multiple pass experiments using high shear

**Table 1 – A summary of the key theoretical correlations to predict mean droplet size, adapted from Leng and Calabrese (2004) and Padron (2005).**

| Range | Mechanism | Correlation in terms of $\varepsilon$ | Correlation in terms of dimensionless groups (constant Po) |
|---|---|---|---|
| $\eta_K > d$ | Inertial stresses; $\mu_d \to 0; \tau_s \gg \tau_v$ | $d_{max} \propto \left(\frac{\sigma\mu_c}{\rho c^2}\right)^{1/3} \varepsilon^{-1/3}$ (7) | $\frac{d_{32}}{D} \propto (WeRe)^{-1/3}$ (8) |
| $\eta_K \gg d$ | Inertial stresses; $\mu_d \to 0; \tau_s \gg \tau_v$ | $d_{max} \propto \left(\frac{\sigma\mu_c^4}{\rho c^5}\right)^{1/7} \varepsilon^{-2/7}$ (9) | $\frac{d_{32}}{D} \propto (WeRe^4)^{-1/7}$ (10) |
| $\eta_K > d$ | Viscous stresses; $\mu_d \to 0; \tau_s \gg \tau_v$ | $d_{max} \propto (\rho_c\mu_c)^{-1/2} \varepsilon^{-1/2}$ (11) | $\frac{d_{32}}{D} \propto (We^{-1}Re^{1/2})$ (12) |

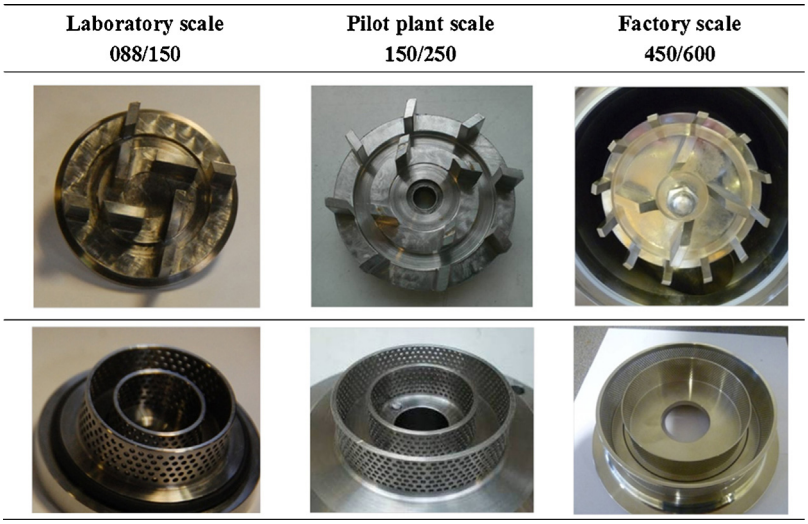


**Fig. 1 – Double rotors and double emulsor stators used in the laboratory scale, pilot plant scale and factory scale mixers.**

dissolver disks and were pumped to the mixer with flow rate measured by a Coriolis flow meter.

### 2.2. Materials

In all three mixers, emulsification of 1 wt.% silicone oils (Dow Corning 200 fluid) with viscosities of 9.4 and 339 mPa s in water was investigated, and all emulsions were stabilised by 0.5 wt.% of sodium laureth sulfate (SLES, Texapon N701, Cognis UK Ltd.).

The effect of interfacial tension on drop size was only investigated in the pilot plant scale (150/250) mixer, with and without surfactant. For the surfactant systems, SLES was used at three concentrations of 0.05, 0.5 and 5 wt.%. In non-surfactant systems, interfacial tension was modified by using aqueous solutions of absolute ethanol (99.8%, VMR

**Table 2 – Dimensions of the laboratory scale, pilot plant scale and factory scale in-line Silverson rotor–stator mixers fitted with double standard emulsor stators.**

| Parameters | Laboratory scale 088/150 | Pilot plant scale 150/250 | Factory scale 450/600 |
|---|---|---|---|
| Inner rotor diameter, $D_{r,i}$ (mm) | 22.4 | 38.1 | 114.3 |
| Outer rotor diameter, $D_{r,o}$ (mm) | 38.1 | 63.5 | 152.4 |
| Inner rotor blades, $n_{b,i}$ | 4 | 4 | 4 |
| Outer rotor blades, $n_{b,o}$ | 4 | 8 | 12 |
| Rotor height, $h_r$ (mm) | 11.10 | 11.91 | 31.75 |
| Swept rotor volume, $V_H$ ($mm^3$) | 12,655 | 37,726 | 579,167 |
| Inner stator diameter, $D_{s,i}$ (mm) | 22.71 | 38.58 | 114.6 |
| Outer stator diameter, $D_{s,o}$ (mm) | 38.58 | 63.98 | 152.7 |
| Outer stator height, $h_s$ (mm) | 14.33 | 16.66 | 32.56 |
| Inner stator | | | |
| *Number of holes, $n_h$* | *180* | *300* | *2016* |
| *Rows, $n_r$* | *6* | *6* | *14* |
| *Holes per row, $n_{hr}$* | *30* | *50* | *144* |
| Outer stator | | | |
| *Number of holes, $n_h$* | *240* | *560* | *2496* |
| *Rows, $n_r$* | *5* | *7* | *13* |
| *Holes per row, $n_{hr}$* | *48* | *80* | *192* |
| Outer stator perimeter of openings, $P_h$ (mm) | 1197 | 2793 | 12,448 |
| Outer stator screen area, $A_s$ ($mm^2$) | 12,655 | 37,726 | 579,167 |
| Outer stator open area, $A_h$ ($mm^2$) | 1736- | 3349 | 15,620 |
| Fraction of outer stator open area, $A_F$ (%) | 27.4 | 33.1 | 31.6 |
| Maximum rotor speed, $N$ (rpm) | 10,000 | 12,000 | 3600 |
| Maximum (nominal) flow rate, $M$ ($kg\,h^{-1}$) | 1500 | 6200 | 6200 |

International Ltd) at concentrations of 0, 10 and 20 wt.%. as the continuous phase.

The interfacial tensions were measured by the Wilhelmy plate method using the Kruss Easydrop (VI-03) Drop Shape Analysis System at ~22 °C. Interfacial tension falls from 40.9 to 26.6 and 17.7 mN m$^{-1}$ as the concentration of ethanol increases from 0 to 10 and 20 wt.% respectively. An increase of SLES concentration from 0.05 to 0.5 and 5 wt.% lead to a reduction of interfacial tension from 13.8 to 10.0 and 7.3 mN m$^{-1}$ respectively.

### 2.3. Emulsification

Emulsification was carried out in two steps. First coarse emulsion was prepared in a stirred vessel that was further emulsified in a rotor–stator mixer.

The coarse emulsions were prepared in a mixing vessel at a constant temperature of 25 ± 1 °C, and where necessary stabilised with SLES. For the aqueous ethanol continuous phases, ethanol was added slowly to the water on the surface with no agitation, then mixed thoroughly. Silicone oil was added to the mixing tank at 1 wt.% phase volume and the dispersion was agitated to give average drop sizes between 45 and 50 μm. Throughout all experiments, coarse emulsions were mixed at low speed to maintain a well-mixed dispersion and prevent creaming.

The effect of rotor speed (energy dissipation rate), flow rate, viscosity of the dispersed phase and interfacial tension on drop size distributions in high shear mixers were investigated for both single and multiple pass emulsification.

#### 2.3.1. Single pass

Coarse emulsion was fed to the Silverson at a range of flow rates and rotor speeds. For the pilot plant scale 150/250 mixer, rotor speeds from 3000–11,000 rpm (in steps of 1000 rpm) at a primary flow rate of 300 kg h$^{-1}$, and rotor speeds of 6000 rpm and 11,000 rpm for flow rates between 150 and ~6200 kg h$^{-1}$ were examined. Ethanol continuous phase systems were emulsified at 3000–11,000 rpm (in steps of 2000 rpm) at a flow rate of 300 kg h$^{-1}$. The primary flow rates for the laboratory scale 088/150 and factory scale 450/600 mixers were roughly 100 kg h$^{-1}$ and 4600 kg h$^{-1}$ respectively, to match the residence time in the pilot plant scale 150/250 mixer of $\tau = 0.45$ s.

Drop size distributions in the mixing tanks, after the pump and at the Silverson inlet were practically identical, e.g. no breakage was observed in the pump.

#### 2.3.2. Multiple passes

The effect of multiple passes on droplet size distributions was investigated by two methods; 'single condition' recirculation, and 'step-wise' recirculation methods, both using the 60 L rig. In the 'single condition' method, coarse emulsion was fed to the Silverson mixer in a recycle loop between the mixing tank and the mixer. Flow rate and rotor speed were kept constant with samples taken from the Silverson outlet at regular time intervals corresponding to a given number of batch turnovers.

Initially, coarse emulsion was circulated around the system at a low flow rate (300 kg h$^{-1}$) to remove air from the pipelines, then the Silverson was turned to the required rotor speed, and the flow rate was controlled by direct adjustment of the pump and the valve at the mixer outlet.

In 'step-wise' recirculation, the emulsion was recycled for 1 h to obtain an 'equilibrium' droplet size distribution. For each run, flow rate was constant and rotor speed increased in steps, with samples taken from the Silverson outlet at regular time intervals. This method examined the effect of processing at long times, although in reality droplet size never reached an 'equilibrium', but a time of 1 h was selected as this was considerably longer than manufacturing timescales. The flow rates were varied between 300 kg h$^{-1}$ and 3600 kg h$^{-1}$ and rotor speed between 3000 rpm and 11,000 rpm. In selected runs, residence times and tip speeds were the same in all three mixers.

#### 2.3.3. Measurements of drop size distributions

Droplet size distributions were measured using a Mastersizer 2000 particle analyser (Malvern Instruments, Malvern, UK). Samples were diluted in a ~0.1 wt.% SLES solution to prevent coalescence and oil deposition on the optical windows of the sample cell. The relative refractive indices used were 1.33 for water, and 1.42 for silicone oil. The imaginary component of the absorption index for silicone oil was taken as 0.001 (Thapar, 2004). In general, samples were measured <48 h after the experiment was completed, although the samples were stable over a longer period of time.

The results of the measurements are presented as drop size distributions supported by the calculated span describing the width of distributions (Seville et al., 1997):

$$w = \sqrt{\frac{d_{0,9}}{d_{0,1}}} \tag{17}$$

and skewness (Vanoni, 2006):

$$s = \frac{\ln(\sqrt{(d_{0,9} \cdot d_{0,1})}/d_{0,5})}{\ln(w)} \tag{18}$$

Skewness measures the asymmetry of the drop size distribution and can be positive or negative. Negative skewness indicates that the tail on the left side of the drop size distribution is longer than the right side, and positive skewness indicates that the tail on the right side is longer than the left side and the bulk of the values lie to the left of the mean. The coefficient of determination ($R^2$) was used as the fit indicator in correlations developed from experimental data (power consumption as a function of process parameters and Sauter mean diameter as a function of selected parameters, see Section 3.2). Adjustable parameters in correlations were determined in Microsoft Excel.

### 2.4. Power draw

For turbulent power draw measurements, the 800 L tank was filled with water at ambient temperature and overflowed to maintain a constant head. For the pilot plant scale 150/250 Silverson mixer, water was then fed into the mixer at rotor speeds from 3000 rpm to 11,000 rpm in steps of 1000 rpm. Temperature differences were measured over a series of flow rates from 300 kg h$^{-1}$ to the maximum possible using the rig configuration (~6200 kg h$^{-1}$ at 11,000 rpm). At steady state conditions, when flow rate/pressure, rotor speed and temperature were constant, flow rate, temperature and pressure measurements were recorded for > 5 minutes.

For the factory scale 450/600 mixer, power was measured for a matrix of conditions at rotor speeds from 1200 rpm to 3600 rpm in steps of 600 rpm, at flow rates from 1200 kg h$^{-1}$ to ~6200 kg h$^{-1}$. Power of the laboratory scale 088/150 mixer was only measured at higher rotor speeds of 8000 rpm and

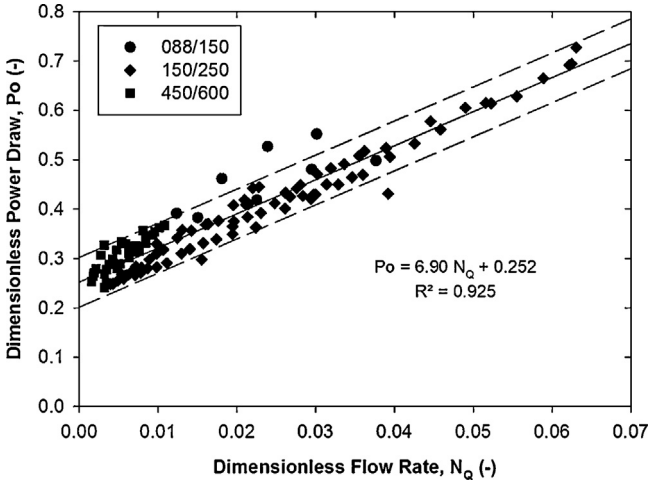


**Fig. 2 – Dimensionless power draw as a function of dimensionless flow rate for three scales of in-line Silverson mixer, with 20% error lines.**

10,000 rpm where larger temperature differences could be produced, at flow rates of 200 kg h$^{-1}$ to ~1500 kg h$^{-1}$ (Hall, 2013).

At steady state conditions, power draw was estimated from the temperature difference between the mixer inlet and outlet ($\Delta\theta$) (Ascanio et al., 2004):

$$P = MC_p(\Delta\theta) \quad (19)$$

Systematic temperature differences between the thermocouples and power consumed due to pumping were accounted for as discussed by Kowalski et al. (2011). A pressure drop term, was included in power draw, (see Kowalski et al., 2011 for details) and the total power was calculated from:

$$P = MC_p(\Delta\theta - \theta_c) - MC_p(\Delta\theta_b - \theta_c) + Q(\Delta p) \quad (20)$$

The power calculated from this equation (based on experimental results) was used to calculate the constants in the theoretical expression for power draw (Eq. (1)) and the standard error.

## 3. Results and discussion

### 3.1. Power draw

The power constants for three scales of in-line Silverson rotor–stator mixer were obtained from multi-linear regression. Values of $Po_Z$ are roughly scale independent and equal ~0.24 (0.254, 0.229 and 0.231 for the lab, pilot plant and factory mixers, respectively) with standard error ranging from 0.004 at the pilot plant scale to 0.034 at the lab scale. The highest standard error at the smallest scale was caused by the smallest difference of temperature during the measurement of power consumption. The flow power constant ($k_1$) is 9.59, 7.46 and 11.80 in the lab, pilot plant and factory mixers, respectively. Since both $Po_Z$ and $k_1$ are similar at each scale, this confirms that the modified expression for power draw can be used to calculate power draw at different scales of in-line Silverson mixer from:

$$P = 0.252\rho N^3 D^5 + 6.90MN^2D^2 \quad R^2 = 0.925 \quad (21)$$

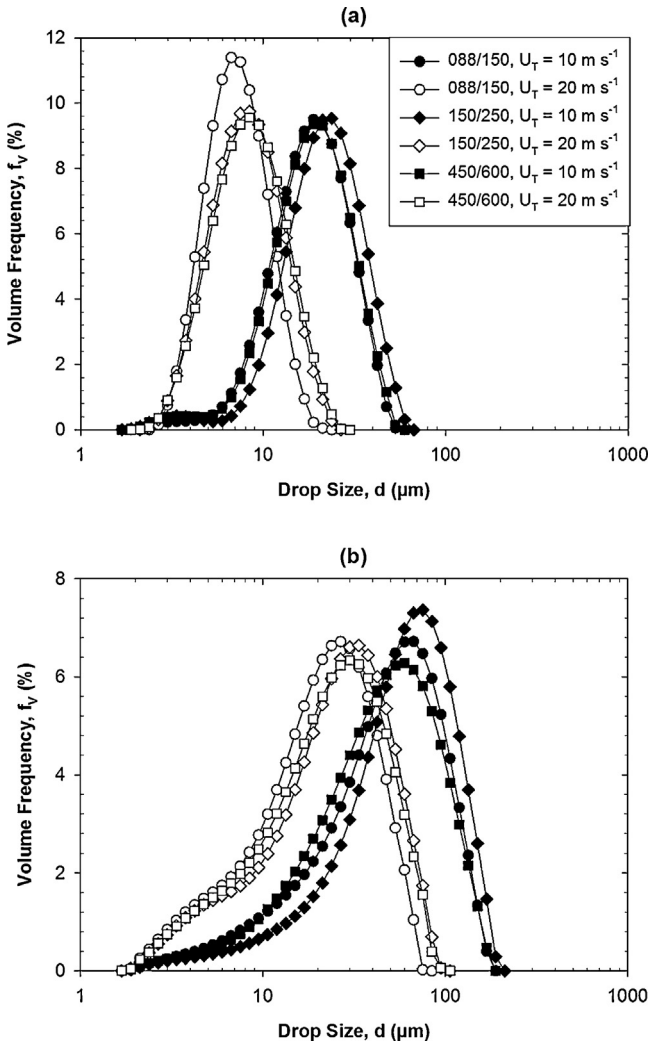


**Fig. 3 – Volume drop size distributions at tip speeds of 10 and 20 m s$^{-1}$ for three mixer scales for 1% (a) 9.4 mPa s and (b) 339 mPa s silicone oil emulsions at a constant residence time of 0.45 s.**

The dimensionless power draw as a function of the dimensionless flow rate shown in Fig. 2 clearly indicates that Eq. (21) correlates the experimental data within +/− 20%, accuracy which is more than sufficient for engineering calculations.

### 3.2. Single pass emulsification

The effects of the mixer scale, dispersed phase viscosity and rotor tip speed on drop size distributions are summarised in Fig. 3. For low viscosity oil at the higher tip speed (20 m s$^{-1}$), drop size distributions were practically log-normal (Fig. 3a) with a (log-normal) span of 1.6–1.8 for all three mixers. At the lower tip speed of 10 m s$^{-1}$, a tail appeared on the left of the DSD and as a result, span increased slightly to 1.85.

As expected, the volume of oil in the smaller drops is reduced at the lower tip speed; however the DSDs have very much the same shape for all scales, with skewness close to zero (−0.09–0.02).

The high viscosity oil drop size distributions at each scale were again rather similar; however they were not log-normal but strongly skewed towards smaller drops (Fig. 3b). At the higher tip speed (20 m s$^{-1}$), span was higher than for the low viscosity oil at 2.7–2.9, and at 10 m s$^{-1}$, span was similar at

**Table 3 – Coefficients from non-linear regressions for correlations of $d_{32}$ with scale-up terms ($d_{32}/D$ with $We$) for two viscosities, at three mixer scales at a constant residence time of 0.45 s.**

| | Results from regression | | | |
|---|---|---|---|---|
| | $b$ | $A$ | $R^2$ | $\sigma_{rms}$ (%) |
| 9.4 mPa s | | | | |
| $\varepsilon$ | −0.39 | 207 | 0.931 | 14.3 |
| $\varepsilon_T$ | −0.34 | 132 | 0.878 | 16.8 |
| $U_T$ | −1.13 | 212 | 0.974 | 8.1 |
| $We$ | −0.70 | 0.63 | 0.956 | 18.9 |
| 339 mPa s | | | | |
| $\varepsilon$ | −0.33 | 255 | 0.899 | 17.4 |
| $\varepsilon_T$ | −0.29 | 172 | 0.838 | 17.2 |
| $U_T$ | −0.98 | 273 | 0.971 | 7.6 |
| $We$ | −0.66 | 0.76 | 0.922 | 25.9 |

2.5–2.8. The small drops form a long tail resulting in a negative skewness of −0.19 to −0.28 at all scales.

In general, these figures show very good agreement in the shape of the distributions between the scales, and as expected, smaller drops are produced in dispersion of the lower viscosity oil. The maximum drop size at all scales (for a given tip speed and viscosity) are very similar, indicating that drop breakage mechanisms are also similar.

### 3.2.1. *Drop size correlations*

Single pass mean drop sizes measured at three scales at the same mean residence time ($\tau = 0.45$ s) were correlated with mean energy dissipation rate, tip speed and Weber number. Mean energy dissipation rate ($\varepsilon$) was calculated from total power draw (Eq. (1)) and also from $P_T = Po_z \rho N^3 D^5$, to give the rotor energy dissipation rate ($\varepsilon_T$) and both forms were examined here. Sauter mean diameters were correlated using the power law model:

$$d_{32} = A_1 * (\text{parameter})^{b_5} \quad (22)$$

or in the case of Weber number:

$$\frac{d_{32}}{D} = A_2 * We^{b_6} \quad (23)$$

Proportionality constants $A$, exponents $b$ and coefficients of determination $R^2$ were calculated by non-linear regression from the experimental data and the results are summarised in Table 3.

Fig. 4a illustrates that the results of the correlations with tip speed give the best fit ($R^2$>0.97 for both oils) and a worse fit for rotor energy dissipation rate in Fig. 4b.

Fig. 4a shows that for both oils, Sauter mean diameters at three scales correlated with tip speed practically fall onto two distinctive straight lines, with high viscosity oil forming systematically larger drops. When rotor energy dissipation rate is used as a correlating parameter the experimental data are scattered and there is even an unphysical overlap between low and high viscosity drops at the lower end of energy dissipation rate.

The exponent on tip speed calculated from the data obtained with low viscosity oil at all scales is very close to the theoretical value for fully developed turbulent flow of −1.2, however at high viscosity oil this is close to −1 which is typical for droplet breakage in simple shear flow.

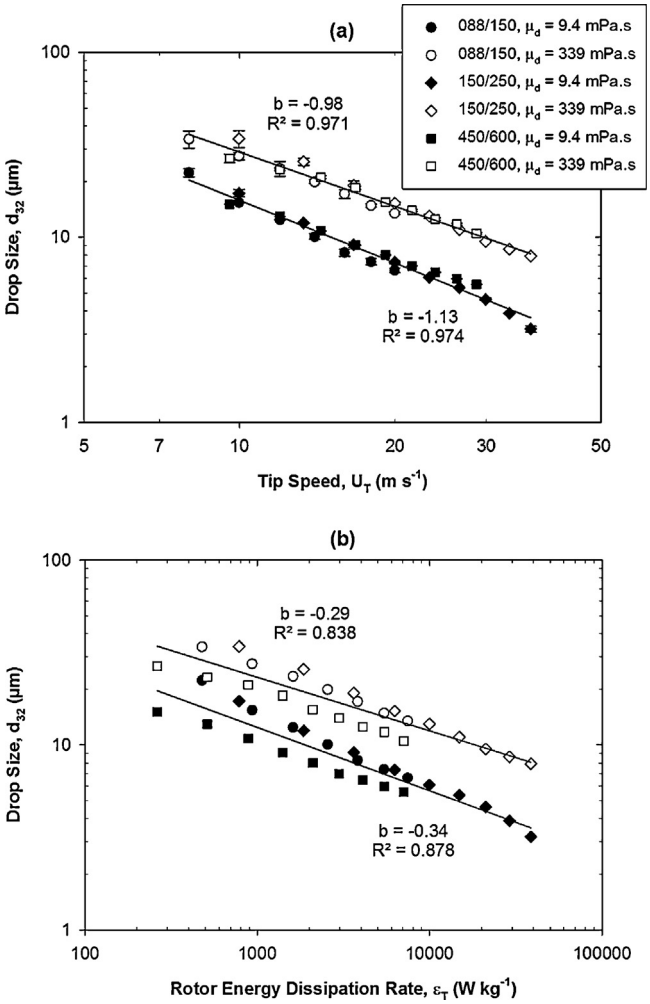


**Fig. 4 – Mean drop size of 1% 9.4 and 339 mPa s silicone oil emulsions as a function of (a) tip speed and (b) rotor energy dissipation rate at three mixer scales, at a constant residence time of 0.45 s.**

The exponents on total energy dissipation rate are close to theoretical values for turbulent flow. The marginal difference in the gradients indicates that at each viscosity and scale, drops are broken by similar mechanisms, primarily by turbulent inertial forces. The substantial differences in the intercepts for each viscosity shows that breakage of low viscosity drops requires less energy than breakage of high viscosity drops. As the coefficients of determination are 0.899 (high $\mu_d$) and 0.931 (low $\mu_d$) (Table 3), it appears that energy dissipation rate does not correlate the data particularly well at different scales. Kamiya et al. (2010b) also used total energy dissipation rate to correlate a pilot plant and a production scale rotor–stator mixer, and reported a similar correlation with $R^2 = 0.91$.

The effect of tip speed on Sauter mean diameter of emulsions shown in Fig. 4a indicates that at the same dispersed phase viscosity, Sauter mean diameters at three different scales fall in one line on logarithmic coordinates. For high viscosity oil, $b = -0.98$ ($R^2 = 0.971$), and for low viscosity oil, $b = -1.13$ ($R^2 = 0.974$), which indicates that tip speed can be treated as a good scaling parameter. Tip speed was a good correlating parameter for dispersion/emulsification in stirred vessels (El-Hamouz et al., 2009).

Dimensionless drop size as a function of Weber number gives a slightly weaker fit than tip speed, with $R^2 = 0.956$ for

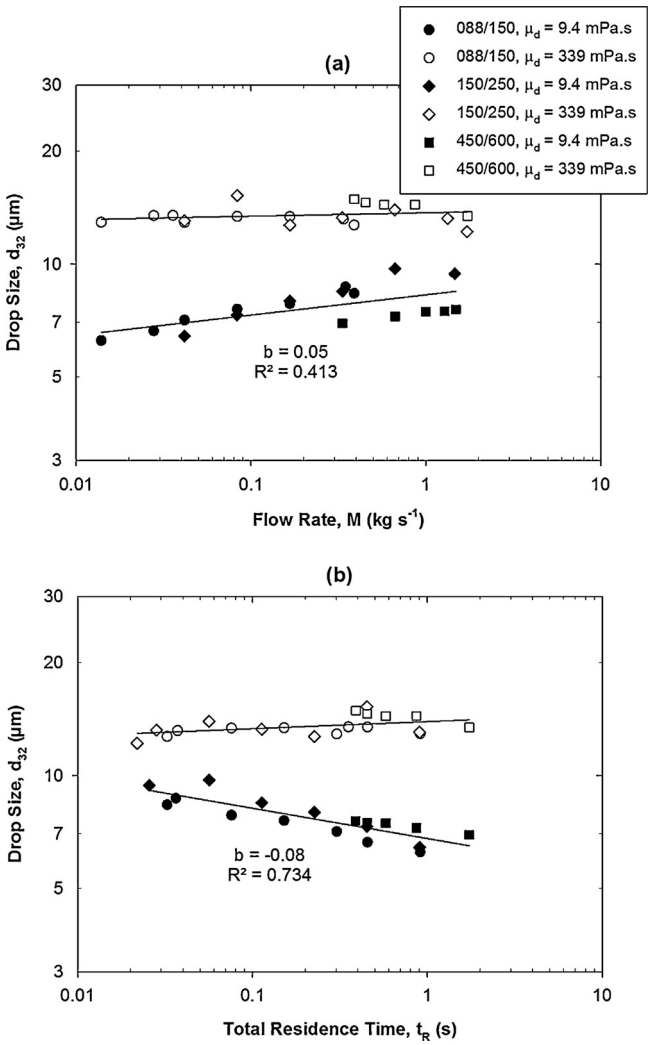


**Fig. 5 – The effect of (a) flow rate and (b) total residence time on mean drop size of 1% 9.4 and 339 mPa s silicone oil emulsions, at a tip speed of 20 m s$^{-1}$ at three mixer scales.**

low viscosity oil and $R^2 = 0.922$ for high viscosity oil. This is expected as in the results discussed above; Weber number is related only to energy dissipation rate as interfacial tension was approximately constant. The effect of interfacial tension on drop size is discussed in Section 3.4.

The above discussion indicates that tip speed appears to be the most appropriate scaling parameter. The poorer applicability of energy dissipation rate as a scaling parameter and the dependency of the exponents on $\varepsilon$ at different scales suggests that the Hinze model cannot be applied to describe droplet break-up in in-line high shear mixers. The suitability of tip speed rather than energy dissipation rate suggests that tip speed is a better approximation of the maximum energy dissipation rate which is important for droplet break-up.

### 3.2.2. *Flow rate and residence time*

The effect of flow rate and mean residence time in the mixer on Sauter mean diameter of emulsions at different scales is shown in Fig. 5.

The Sauter mean diameters of emulsions of viscous drops at all investigated scales are practically independent of flow rate/residence time. Only for low viscosity oil is there a weak dependency of both flow rate and residence time, with residence time giving a better fit to the experimental data. This confirms that accounting for total residence time in the mixing

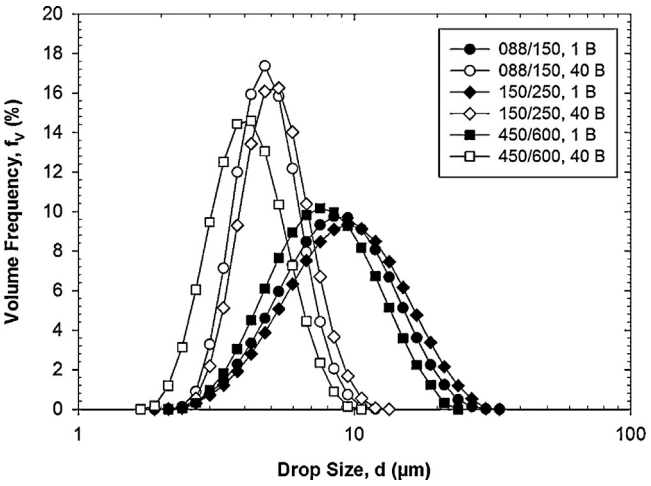


**Fig. 6 – Drop size distributions in three mixers after 1 and 40 batch turnovers, at a tip speed of 20 m s$^{-1}$ for 1% 9.4 mPa s silicone oil emulsions. Residence time ($\tau$) per pass at each scale: laboratory scale (088/150) = 0.0757 s; pilot plant scale (150/250) = 0.0586 s; factory scale (450/600) = 0.8661 s.**

head might improve accuracy of correlations for mean drop size.

### 3.3. *Multiple pass emulsification*

To compare emulsification for both single and multiple passes at different flow rates, residence time was modified to estimate total residence time:

$$t_R = \frac{V_H}{Q} B \tag{24}$$

where the number of vessel turnovers pumped, ($B$) e.g. mean number of passes (Baker, 1996):

$$B = \frac{Q}{V_T} t \tag{25}$$

For a single pass system, $B = 1$.

The effect of number of batch turnovers (1 and 40) and mixer scale on drop size distributions at the mixer outlet are summarised in Fig. 6. For one batch turnover, DSDs were practically log-normal with span ~1.8 for all three scales. After 40 batch turnovers, as expected, the volume of oil contained in small droplets increased, and span reduced to ~1.4.

There is very good agreement in the shape, span and skewness of the distributions between the scales for the same number of batch turnovers, and the maximum and minimum drop sizes are also very similar. At equal energy dissipation rates, smaller drops were produced in the largest mixer and larger drops in the intermediate mixer. This can be attributed to the longest residence time per pass in the largest mixer ($\tau = 0.87$ s), and the shortest time in the medium size mixer ($\tau = 0.06$ s).

### 3.3.1. *Drop size correlations*

Multiple pass emulsification was investigated at several rotor speeds at one flow rate, and the Sauter mean diameters of 9.4 mPa s silicone oil were correlated with energy dissipation rate, energy density and tip speed after 40 batch turnovers.

Fig. 7 shows that Sauter mean diameter at all three scales correlates well with tip speed ($R^2$ of 0.949), which confirms

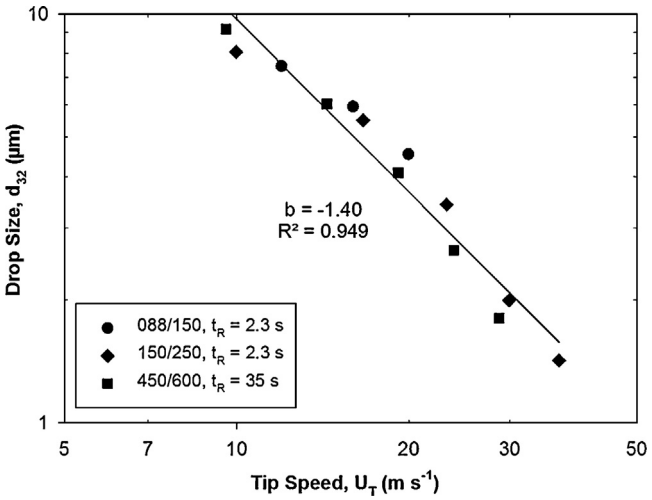


**Fig. 7 – Mean drop size as a function of tip speed of 1% 9.4 mPa s silicone oil emulsions at three mixer scales after 40 batch turnovers.**

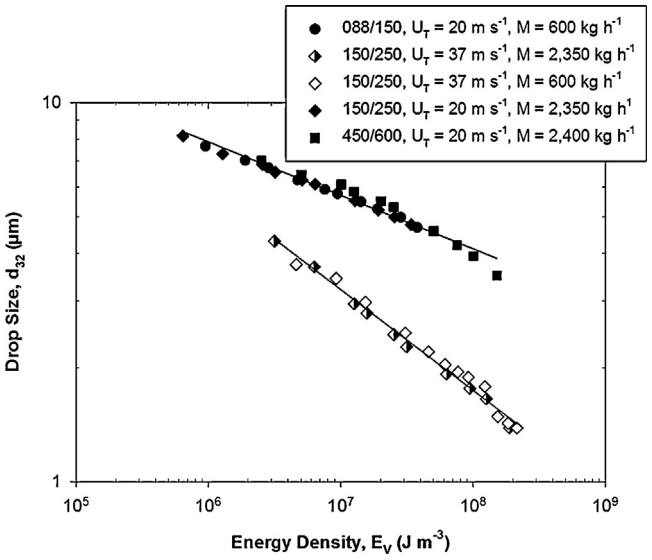


**Fig. 8 – The effect of energy density on mean drop size of 1% 9.4 mPa s silicone oil emulsions, at a tip speed of 20 m $s^{-1}$ at three mixer scales and 37 m $s^{-1}$ for the 150/250 mixer at various flow rates.**

that tip speed is the best scaling parameter for both single and multiple passes.

In Fig. 7, the number of batch turnovers at each scale was 40, however total residence time ($t_R$) was greater at the largest scale at 35 s, compared to 2.3 s at the other scales. To match $t_R$ at other scales, a flow rate of ~36,000 kg $h^{-1}$ was required through the largest mixer which could not be achieved using the existing experimental rig. However, Fig. 7 confirms that the effect of $t_R$ on Sauter mean diameter is marginal as drop sizes from the largest mixer are only slightly smaller than from the other mixers.

Sauter mean diameters did not correlate with energy dissipation rate ($R^2$ = 0.553), or energy density ($R^2$ = 0.764). This was particularly true at the largest scale, and supports previous findings for single passes, that energy dissipation rate or energy density alone are not suitable scaling parameters.

The effect of number of passes at each scale was also assessed at a single rotor speed and flow rate ('single condition' recirculation method). The effect of scale on mean droplet size at the same energy density is shown in Fig. 8.

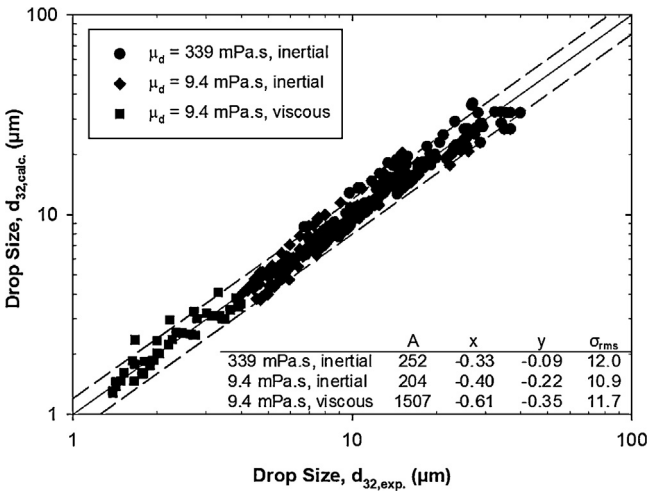


**Fig. 9 – Quality of fit between mean drop size from the correlation presented by Eq. (26) with experimental mean drop size, of 1% 9.4 and 339 mPa s silicone oil emulsions at three mixer scales, with 20% error lines.**

At constant tip speed, energy density correlates drop sizes formed at different residence times, and drop size reduction trends are roughly equal at each scale. However, once tip speed was changed (from 20 m $s^{-1}$ to 37 m $s^{-1}$ for the pilot plant scale 150/250 mixer), energy density does not correlate drop size, which implies that energy density cannot be used for correlation.

### 3.3.2. *Drop size and residence time correlations*

Mean droplet size for continuous emulsification can also be related to energy density (Karbstein and Schubert, 1995), see Eq. (16). Energy density enables comparison of different continuous flow emulsifying devices, and it accounts for both energy dissipation rate and total residence time, however it assumes both terms have the same weight. The poor correlations with energy density discussed above indicate that this might not be the case and that the effect of each term might be different:

$$d_{32} = A_3 \varepsilon^{x_1} t_R^{y_1} \quad (26)$$

Correlation based on tip speed can also be modified in a similar way:

$$d_{32} = A_4 U_T^{x_2} t_R^{y_2} \quad (27)$$

Each of these correlations has a term accounting for the intensity of droplet deformation and a term accounting for the duration of droplet deformation.

Table 4 summarises correlations for mean drop size using Eqs. (26) and (27) for low and high viscosity drops measured at three scales, including single pass and multiple passes, containing about 200 data points. Both correlations are rather accurate with the higher viscosity oil correlating better with Eq. (27), but for lower viscosity oil, differences between the correlations are marginal.

The key difference between the correlations for the two oil viscosities is the change in the exponent x (−1.19 and −0.96) on tip speed and (−0.41 and −0.33) on $\varepsilon$ (Table 4). This follows that the higher oil viscosity is approaching the viscous limit in Eq. (6). Similarly, the exponent y for the higher viscosity oil is 60–70% below the lower viscosity oil exponent.

**Table 4 – Coefficients and constants from non-linear regressions for correlations in Eqs. (26) and (27) for 1% 9.4 and 339 mPa s oil emulsions.**

| Dispersed phase viscosity, $\mu_d$ (mPa s) | Scale-up term | A | x | y | $R^2$ | $\sigma_{rms}$ (%) |
|---|---|---|---|---|---|---|
| 339 | $\varepsilon^x t_R^y$ | 252 | −0.327 | −0.090 | 0.901 | 12.0 |
| 339 | $U_T^x t_R^y$ | 233 | −0.957 | −0.043 | 0.944 | 8.3 |
| 9.4 | $\varepsilon^x t_R^y$ | 219 | −0.409 | −0.228 | 0.938 | 17.0 |
| 9.4 | $U_T^x t_R^y$ | 206 | −1.190 | −0.148 | 0.940 | 22.4 |

Overall, the correlations based on either tip speed or energy dissipation rate give a reasonable prediction of mean drop size when total residence time is included. However, y is greater for the correlation with $\varepsilon$ than $U_T$, as y compensates for the poorer applicability of $\varepsilon$ as a scaling parameter, discussed in Section 3.2.

The energy dissipation rate correlations in Table 4 are shown in Fig. 9. Once mean drop sizes for 9.4 mPa s oil emulsions are separated, correlation of the larger drop sizes $>\eta_K$ fit exactly with an exponent of −0.40 on energy dissipation rate, while for the smaller drops $<\eta_K$ an exponent of −0.61 has been found. This adds further support to the fact that droplets below $\eta_K$ correlate with an exponent of >0.5 on $\varepsilon$.

### 3.4. *Effect of interfacial tension on scale-up parameters*

The interfacial tension between two immiscible liquids strongly affects drop size and it is included in Weber number, so investigation of this physical property further examines the applicability of Weber number as a scaling parameter. All experiments reported in this section were single passes through the pilot plant scale 150/250 mixer.

#### 3.4.1. *Non-surfactant systems*

Mean size of oil drops emulsified in ethanol solutions as a function of energy dissipation rate are shown in Fig. 10a and dimensionless Sauter mean diameters as a function of Weber number in Fig. 10b. As expected, smaller droplets were formed at a lower interfacial tension (for both viscosities) because a lower interfacial tension reduces the surface force which resists droplet break-up. Mean drop sizes at 27 and 18 mN m$^{-1}$ began to converge at higher energy dissipation rates which are mostly likely due to the coalescence of the smallest droplets formed, as stability against coalescence is reduced for low $\sigma$ systems (Walstra, 2005). Very similar trends were observed for high viscosity oil. The exponents on energy dissipation rate are close to -0.4 indicating turbulent inertial droplet break-up in all cases.

Fig. 10b shows that Weber number accounts well for the effect of interfacial tension for non-surfactant systems, collapsing results in two lines corresponding to low and high dispersed phase viscosities which suggests that Weber number is suitable as a scaling parameter. The exponents are slightly lower than the theoretical −0.6 value for turbulent inertial break-up, which is particularly evident at higher Weber numbers for interfacial tensions of 18 mN m$^{-1}$.

#### 3.4.2. *Surfactant systems*

The mean drop size of emulsions containing 0.05 wt.% ($\sigma$ = 13.8 mN m$^{-1}$), 0.5 wt.% ($\sigma$ = 10 mN m$^{-1}$), 5 wt.% ($\sigma$ = 7.3 mN m$^{-1}$) SLES as a function of energy dissipation rate are shown in Fig. 11a and dimensionless Sauter mean diameters as a function of Weber number in Fig. 11b. Fig. 11a shows that smaller drops were formed at a slightly lower

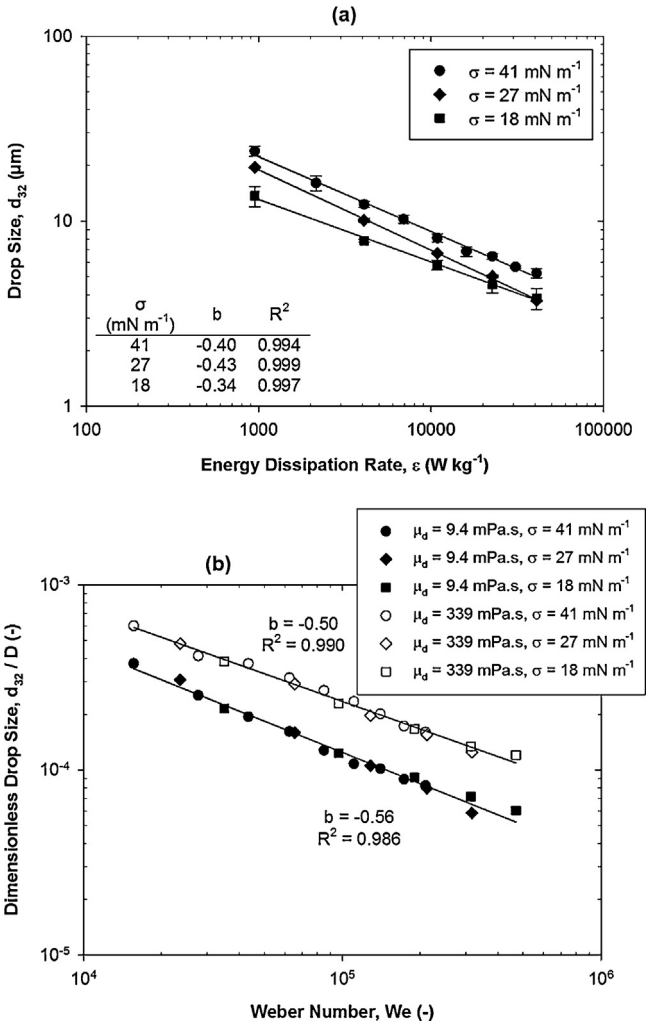


**Fig. 10 – (a) Mean drop size as a function of energy dissipation rate of 1% 9.4 mPa s silicone oil emulsions with standard deviation error bars (b) and dimensionless drop size as a function of Weber number of 9.4 and 339 mPa s silicone oil emulsions in the 150/250 mixer at 300 kg h$^{-1}$.**

interfacial tension (7.3 mN m$^{-1}$ for 5 wt.% SLES compared to 13.8 mN m$^{-1}$ for 0.05 wt.% SLES) (for both viscosities of silicone oil investigated). In general there was little effect of surfactant concentration on mean drop size despite the 100-fold increase in SLES content, and in all cases the gradients are close to −0.4.

For high viscosity oil dispersed in 5 wt.% SLES, smaller drops were obtained at lower energy dissipation rates, giving a shallower gradient (−0.28) on $\varepsilon$, compared to the other SLES concentrations. The concentration of SLES has little effect on the shape or position of the distributions with the highest surfactant concentration forming slightly smaller droplets.

Correlating drop size with Weber number based on interfacial tension leads to different trend lines not only for different viscosities but also for non-surfactant and surfactant systems

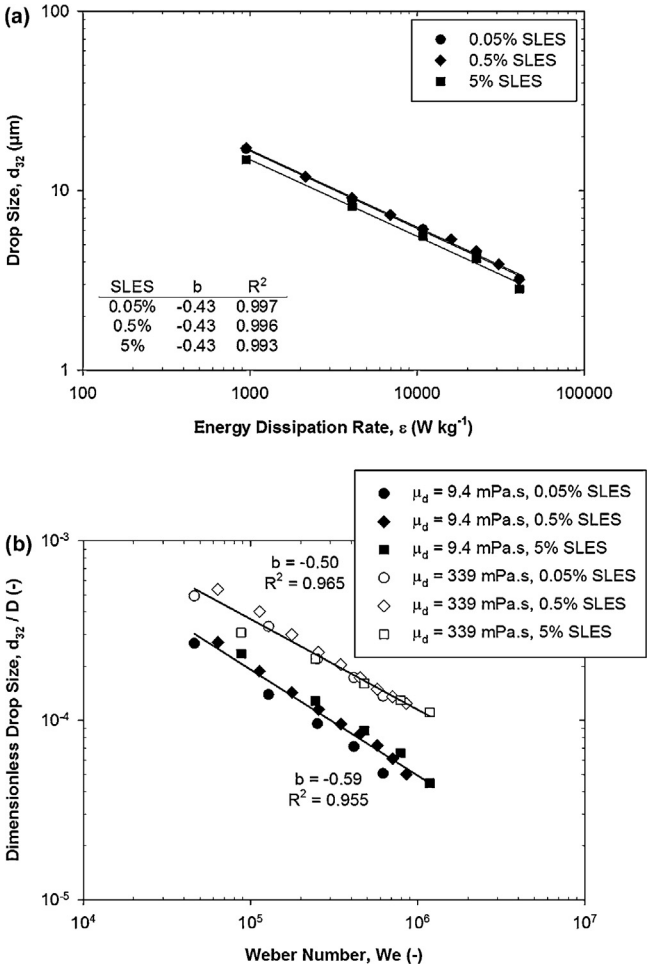


**Fig. 11 – Mean drop size at 0.05 wt.%, 0.5 wt.% and 5 wt.% SLES as a function of energy dissipation rate of (a) 1% 9.4 mPa s silicone oil emulsions with standard deviation error bars and (b) dimensionless drop size as a function of Weber number for 9.4 and 339 mPa s silicone oil emulsions.**

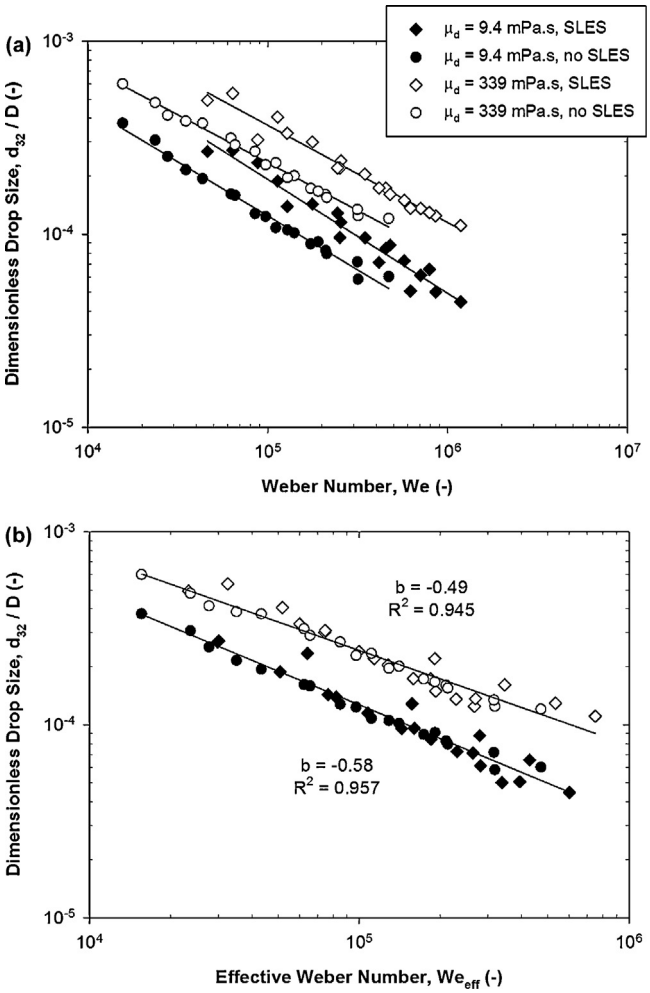


**Fig. 12 – Dimensionless mean drop size of 1% 9.4 and 339 mPa s silicone oil emulsions in ethanol and surfactant solutions as a function of (a) Weber number and (b) effective Weber number, in the 150/250 mixer at 300 kg h$^{-1}$.**

(Fig. 12a). Janssen et al. (1994) proposed that for surfactant systems, effective interfacial tension, which depends on the surface excess ($\Gamma$) at the oil–water interface, should be used instead of interfacial tension:

$$\sigma_{eff} = \sigma + \beta E_{sd} \tag{28}$$

They found Weber number to increase with surfactant concentration, corresponding to the surface dilational modulus ($E_{sd}$) and proposed the use of effective interfacial tension ($\sigma_{eff}$). The surface dilational modulus is a system property and relates the change of the interfacial tension resulting from a change in the interfacial area of the drop (Walstra and Smulders, 1998):

$$E_{sd} \approx \frac{E_0}{1 + (t_D/t_{def})^{-1/2}} \tag{29}$$

where $E_0$ is the limiting elasticity of the interface:

$$E_0 = \frac{-d(\sigma)}{d \ln \Gamma} \tag{30}$$

The surface excess ($\Gamma$) at the oil–water interface depends on the bulk concentration of surfactant in the continuous phase.

At lower surfactant concentrations, interfacial tension gradients form on the droplet surface when the droplet is deformed, which results in Marangoni stresses resisting droplet disruption. At high surfactant concentrations, the diffusion time of surfactant from the bulk to the droplet interface decreases, and the Marangoni stresses are reduced, hence this phenomena is less important at high surfactant concentrations, or in non-surfactant systems.

Measurement/calculation of surface excess is rather complex therefore $\Gamma$ determined for SDS (Walstra and Smulders, 1998) were used giving 0.5 mg m$^{-3}$ for 0.05 wt.% SLES and 0.7 mg m$^{-3}$ for 0.5 wt.% and 5 wt.% SLES. The value of $t_D$ was also taken for SDS as $1 \times 10^{-10}$ m$^2$ s$^{-1}$ (Yang and Matthews, 2000), and the droplet deformation time was calculated for turbulent inertial flow:

$$t_{def} = \frac{\mu_d}{\varepsilon^{2/3} d^{2/3} \rho_c} \tag{31}$$

The constant $\beta$ in Eq. (28) was obtained by fitting the dimensionless mean drop sizes to the Weber number correlation, to give 0.21 ($\sigma_{rms}$ = 10.5%) and 0.58 ($\sigma_{rms}$ = 13.7%) for 9.4 mPa s and 339 mPa s oil respectively, which compares to 0.19–0.26 by Janssen et al. (1994).

The effective Weber number was calculated from:

$$We_{eff} = \frac{\rho_c N^2 D^3}{\sigma_{eff}} \tag{32}$$

Fig. 12b shows that introducing effective interfacial tension in the Weber number correlation for surfactant systems, brings together mean drop sizes of emulsions measured in non-surfactant and surfactant systems and confirms that effective interfacial tension can correlate surfactant and non-surfactant systems, however this approach should be verified using a range of surfactants.

## 4. Conclusions

For the first time in open literature the results of very detailed scale-up studies of in-line Silverson rotor–stator mixers are reported. The experiments were carried out using lab, pilot plant and full industrial scale in-line Silverson rotor–stator mixers and both power draw and emulsification were investigated over wide range of processing conditions. It was found that for all three scales, power draw is the sum of the rotor and flow contributions, with proportionality constants, $Po_Z$ and $k_1$, that are practically scale independent.

During emulsification, drop size distributions at three scales are practically identical, which suggests that the droplet breakage mechanism was very similar. For single pass systems, and the same residence time in the mixing head, tip speed was found to be the best scaling parameter.

Energy dissipation rate is also a reasonable scaling parameter, however the suitability is reduced when total residence time was not constant. Application of the rotor energy dissipation rate which neglects power due to the flow rate produced a less favourable correlation. The effect of number of passes was successfully correlated with energy dissipation rate and total residence time. The experimentally determined exponent on energy dissipation rate compared well with theoretical models for turbulent inertial stresses.

Weber number accounts well for the effect of interfacial tension on drop size in surfactant free systems but in presence of surfactant, effective interfacial tension containing an elasticity term gives better agreement with experimental results.

## Acknowledgements

The authors would like to acknowledge the Engineering and Physical Sciences Research Council (ESPRC) and Unilever for EngD funding, and the Royal Commission for the Exhibition of 1851 for the Industrial Fellowship for S. Hall, the Royal Society of the UK for the Industry Fellowship for Prof. A. J. Kowalski, and the support by a further research grant from Unilever for Dr M. Cooke. The authors would also like to acknowledge The University of Manchester's School of Chemical and Analytical Science workshop staff and Unilever R&D Port Sunlight engineering workshop for help with modifications and maintenance of the equipment. Finally, the authors acknowledge Dr M. Baker (Unilever) for his work in developing the small scale mixer.

## References

Ascanio, G., Castro, B., Galindo, E., 2004. Measurement of power consumption in stirred vessels – a review. Chem. Eng. Res. Des. 82 (A9), 1282–1290.

Atiemo-Obeng, V.A., Calabrese, R.V., 2004. Rotor–stator mixing devices. In: Paul, E.L., Atiemo-Obeng, V.A., Kresta, S.M. (Eds.), Handbook of Industrial Mixing: Science and Practice. John Wiley & Sons, Inc, Hoboken, NJ, USA, pp. 479–505.

Baker, M.R., 1996. Mixed flow hydrodynamics. In: Cheremisinoff, N.P. (Ed.), Advances in Engineering Fluid Mechanics Series. Gulf Publishing Company, Houston, USA.

Baldyga, J., Bourne, J.R., Pacek, A.W., Amanullah, A., Nienow, A.W., 2001. Effects of agitation and scale-up on drop size in turbulent dispersions: allowance for intermittency. Chem. Eng. Sci. 56, 3377–3385.

Baldyga, J., Kowalski, A., Cooke, M., Jasinska, M., 2007. Investigations of micromixing in a rotor–stator mixer. Chem. Process Eng. 28, 867–877.

Calabrese, R.V., Francis, M.K., Mishra, V.P., Phongikaroon, S., 2000. Measurement and analysis of drop size in a batch rotor–stator mixer. In: van den Akker, H.E.A., Derksen, J.J. (Eds.), Proceedings of the 10th European Conference on Mixing. Elsevier Science, Amsterdam, The Netherlands, pp. 149–156, July 2–5, 2000.

Colenbrander, G.W., 2000. Experimental findings on the scale-up behaviour of the drop size distribution of liquid/liquid dispersions in stirred vessels. In: van den Akker, H.E.A., Derksen, J.J. (Eds.), Proceedings of the 10th European Conference on Mixing. Elsevier Science, Amsterdam, The Netherlands, pp. 173–180, July 2–5, 2000.

Cooke, M., Kowlaski, A.J., Naughton, J., 2008. A simple measurement method for determining the constants for the prediction of turbulent power in a Silverson MS 150/250 in-line rotor stator mixer. In: Sixth International Symposium on Mixing in Industrial Process Industries, ISMIP VI, Niagara on the Lake, Niagara Falls, ON, Canada, p. 2008, August 17-21.

Davies, J.T., 1985. Drop sizes of emulsions related to turbulent energy dissipation rates. Chem. Eng. Sci. 40 (5), 839–842.

El-Hamouz, A., Cooke, M., Kowalski, A., Sharratt, P., 2009. Dispersion of silicone oil in water surfactant solution: effect of impeller speed, oil viscosity and addition point on drop size distribution. Chem. Eng. Process. 42 (2), 633–642.

Francis, M.K., 1999. The Development of a Novel Probe for the In Situ Measurement of Particle Size Distributions, and Application to the Measurement of Drop Size in Rotor Stator Mixers. University of Maryland, College Park, MD, USA (PhD Thesis).

Hall, S., Cooke, M., Pacek, A.W., Kowalski, A.J., Rothman, D., 2011. Scaling up of silverson rotor–stator mixers. Can. J. Chem. Eng. 89 (5), 1040–1050.

Hall, S., 2013. Scale-up of Emulsification in In-line Rotor–Stator Mixers. University of Birmingham, Birmingham, UK (EngD Thesis).

Hinze, J.O., 1955. Fundamentals of the hydrodynamic mechanism of splitting in dispersion processes. AIChE J. 1 (3), 289–295.

Janssen, J.J.M., Boon, A., Agterof, W.G.M., 1994. Influence of dynamic interfacial properties on droplet break-up in simple shear flow. AIChE J. 40 (12), 1929–1939.

Kamiya, T., Kaminoyama, M., Nishi, K., Misumi, R., 2010a. Scale-up factor for mean drop diameter in batch rotor–stator mixers. J. Chem. Eng. Jpn. 43 (4), 326–332.

Kamiya, T., Sugawara, T., Sasaki, H., Tomita, T., Kaminoyama, M., Nishi, K., Misumi, R., 2010b. Scale-up factor for mean drop diameter in batch rotor–stator mixers with internal circulation. J. Chem. Eng. Jpn. 43 (9), 737–744.

Karbstein, H., Schubert, H., 1995. Developments in the continuous mechanical production of oil-in-water macro-emulsions. Chem. Eng. Process. 34, 205–211.

Kowalski, A.J., 2009. An expression for the power consumption of in-line rotor–stator devices. Chem. Eng. Process. 48, 581–585.

Kowalski, A.J., Cooke, M., Hall, S., 2011. Expression for turbulent power draw of an in-line Silverson high shear mixer. Chem. Eng. Sci. 66 (3), 241–249.

Leng, D.E., Calabrese, R.V., 2004. Immiscible liquid–liquid systems. In: Paul, E.L., Atiemo-Obeng, V.A., Kresta, S.M. (Eds.), Handbook of Industrial Mixing: Science and Practice. John Wiley & Sons, Inc, Hoboken, NJ, USA, pp. 639–753.

Maa, Y.-F., Hsu, C., 1996. Liquid–liquid emulsification by rotor/stator homogenization. J. Control. Release 38, 219–228.

Okufi, S., Perez de Ortiz, E.S., Sawistowski, H., 1990. Scale up of liquid–liquid dispersions in stirred tanks. Can. J. Chem. Eng. 68, 400–406.

Pacek, A.W., Chamsart, S., Nienow, A.W., Bakker, A., 1999. The influence of impeller type on mean drop size and drop size distribution in an agitated vessel. Chem. Eng. Sci. 54, 4211–4222.

Padron, G.A., 2005. Effect of Surfactants on Drop Size Distribution in a Batch Rotor–Stator Mixer. University of Maryland, College Park, MD, USA (PhD. Thesis).

Schubert, H., Engel, R., 2004. Product and formulation engineering of emulsions. Chem. Eng. Res. Des. 82 (A9), 1137–1143.

Seville, J.P.K., Tuzun, U., Clift, R., 1997. Processing of Particle Solids. Chapman and Hall, London, UK.

Thapar, N., 2004. Liquid–Liquid Dispersions from In-line Rotor–Stator Mixers. Cranfield University, UK (PhD Thesis).

Vanoni, V.A., 2006. Sedimentation Engineering. American Society of Chemical Engineers, Reston, VA, USA.

Walstra, P., Smulders, P.E.A., 1998. Emulsion formation. In: Binks, B.P. (Ed.), Modern Aspects of Emulsion Science. The Royal Society of Chemistry, Cambridge, UK.

Walstra, P., 2005. Emulsions. In: Lyklema, J. (Ed.), Fundamentals of Interface and Colloid Science, vol. 5. Academic Press, London, UK.

Yang, X., Matthews, M.A., 2000. Diffusion coefficients of three organic solutes in aqueous sodium dodecyl sulfate solutions. J. Colloid Interface Sci. 229, 53–61.